Optics Communications 291 (2013) 253–258

Contents lists available at SciVerse ScienceDirect

Optics Communications

journal homepage: www.elsevier.com/locate/optcom

Classical analogs of double electromagnetically induced transparency

Zhengyang Bai, Chao Hang, Guoxiang Huang *

State Key Laboratory of Precision Spectroscopy and Department of Physics, East China Normal University, Shanghai 200062, China

ARTICLE INFO

Article history:
Received 23 September 2012
Received in revised form
1 November 2012
Accepted 15 November 2012
Available online 5 December 2012

Keywords:
Double electromagnetically induced transparency
Classical analog
Coupled harmonic oscillators
Coupled RLC circuits

ABSTRACT

Double electromagnetically induced transparency (DEIT) in a four-level atomic system with tripod-type energy-level configuration is modeled by using two classical systems. The first is a set of three coupled harmonic oscillators subject to frictional forces and external drives and the second is a set of three coupled RLC circuits with electric resistors and alternating voltage sources. It is shown that both of the two classical systems have absorption spectra of DEIT similar to that of the four-level tripod-type atomic system. These classical analogies provide simple and intuitive physical description of quantum interference processes and can be used to illustrate experimental observations of the DEIT in quantum systems.

1. Introduction

In recent years, tremendous attention has been paid to the study of electromagnetical induced transparency (EIT) and related quantum interference phenomena in atomic systems [1,2]. By means of the quantum interference induced by a control laser field, the absorption of a probe laser field tuned to a strong one-photon resonance can be largely canceled and hence an initially opaque medium becomes transparent. Furthermore, the control field can greatly modify the dispersive property of the atomic medium, leading to a significant reduction of group velocity of the probe field. In addition, the Kerr nonlinearity of the medium can also be enhanced largely. Based on these striking features, many applications of EIT have been explored, such as highly efficient four-wave mixing, quantum memory, optical switches [1,2], ultraslow optical solitons [3–5], and so on.

Besides the single EIT phenomenon in three-level atomic systems, double electromagnetical induced transparency (DEIT) [6–11] may occur when a four-level atomic system with a tripod-type configuration is exposed to three laser fields that drive three different transitions with one common excited level (see Fig. 1). In such settings, a single control laser field can modify the absorption and dispersion properties of the other two probe laser fields and produce large Kerr effects, especially cross phase modulations. Such system has also been used to engineer coherent superposition of two ground states, etc., very promising for applications in quantum information processing and quantum computing [12].

We note that the study of quantum-classical analogies in physics has been proved to be very useful in helping to illustrate and understand many fundamental concepts and applicabilities of different physical theories [13]. It is important to note that these analogies bring to light the fact that many quantum and classical phenomena can be described by similar mathematical models, in which there are drastic difference in fundamental concepts. In the past two decades, many classical analogies of different quantum optical systems have been explored, such as stimulated resonance Raman effect [14], vacuum Rabi oscillation [15], and rapid adiabatic passage [16]. In addition, classical analogies of single EIT by using plasmon metamaterials [17,18], superconducting tetrahertz and planar metamaterials [19–21], as well as metal-superconductor hybrid metamaterials [22] have also been reported recently both theoretically and experimentally.

In this paper, we model DEIT in a four-level atomic system with tripod-type energy-level configuration by using two classical (i.e. mechanical and electric) systems. The first is a set of three coupled harmonic oscillators subject to frictional forces and external drives and the second is a set of three coupled RLC circuits with electric resistors and alternating voltage sources. We show that both of the two classical systems have absorption spectra of DEIT similar to that of the four-level tripod-type atomic system. These classical analogies provide simple and intuitive physical description of quantum interference processes and can be used to illustrate experimental observations of the DEIT in quantum optical systems. The present work is related to recent works of the classical analog of EIT [23,24], which however considered either only a single EIT [23], or EIT in a four-level inverted-Y system [24].

The rest of the paper is arranged as follows. In Section 2 a simple description of DEIT in the four-level tripod-type atomic

* Corresponding author. Tel.: +86 21 62233944.
E-mail address: gxhuang@phy.ecnu.edu.cn (G. Huang).

0030-4018/$ - see front matter © 2012 Elsevier B.V. All rights reserved.
http://dx.doi.org/10.1016/j.optcom.2012.11.040

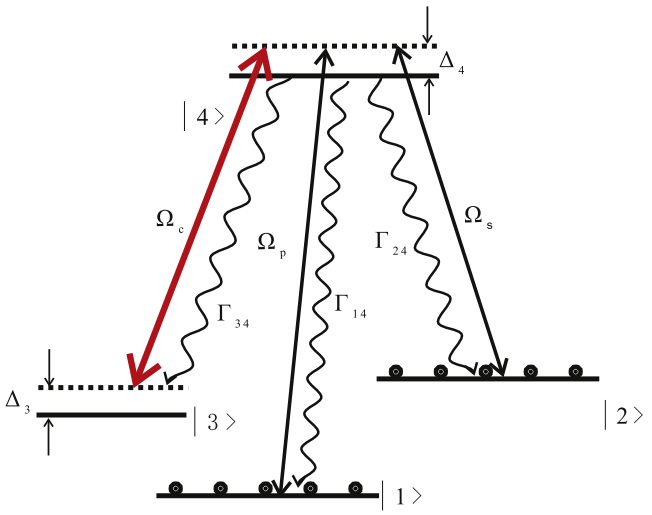

Fig. 1. Energy level structure and excitation scheme of the lifetime-broadened four-level tripod-type atomic system with upper energy level $|4\rangle$ and lower energy levels $|1\rangle$, $|2\rangle$ and $|3\rangle$. Δ_3 and Δ_4 are detunings. Ω_p, Ω_s, and Ω_c are half frequencies of the probe, signal, and control fields, respectively.

system is given. Sections 3 and 4 illustrate the mechanical and electric analogies of DEIT, respectively. The final section summarizes the main results obtained in this work.

2. DEIT in tripod-type atomic system

The DEIT in the four-level tripod-type atomic system has been studied in Refs. [6–11]. Here for completeness we give a simple description of it. Consider a lifetime-broadened four-level atomic system with upper energy level $|4\rangle$ and lower energy levels $|1\rangle$, $|2\rangle$ and $|3\rangle$ (Fig. 1).

A weak probe field of angular frequency ω_p and wavevector $\mathbf{k}_p$, i.e. $\mathbf{E}_p(\mathbf{r},t)=\mathbf{e}_p\mathcal{E}_p(\mathbf{r},t)e^{i(\mathbf{k}_p\cdot\mathbf{r}-\omega_p t)}+\text{c.c.}$, couples to the $|1\rangle\rightarrow|4\rangle$ transition, a strong control field of angular frequency ω_c and wavevector $\mathbf{k}_c$, i.e. $\mathbf{E}_c(\mathbf{r},t)=\mathbf{e}_c\mathcal{E}_c(\mathbf{r},t)e^{i(\mathbf{k}_c\cdot\mathbf{r}-\omega_c t)}+\text{c.c.}$, couples to the $|3\rangle\rightarrow|4\rangle$ transition, and a weak signal field of angular frequency ω_s and wavevector $\mathbf{k}_s$, i.e. $\mathbf{E}_s(\mathbf{r},t)=\mathbf{e}_s\mathcal{E}_s(\mathbf{r},t)e^{i(\mathbf{k}_s\cdot\mathbf{r}-\omega_s t)}+\text{c.c.}$, couples to the $|2\rangle\rightarrow|4\rangle$ transition, respectively. Here $\mathbf{e}_p$, $\mathbf{e}_c$, and $\mathbf{e}_s$ are unit polarization vectors of the probe, control, and signal fields with $\mathcal{E}_p(\mathbf{r},t)$, $\mathcal{E}_c(\mathbf{r},t)$, and $\mathcal{E}_s(\mathbf{r},t)$ are, respectively, their envelope functions. Obviously, the present system consists of two Λ-type EIT schemes, i.e. $|1\rangle-|4\rangle-|3\rangle$ and $|2\rangle-|4\rangle-|3\rangle$.

A practical realization for the present system can be a cold ^{87}Rb atomic gas with states assigned as $|1\rangle=|5^2S_{1/2},F=1,m_F=-1\rangle$, $|2\rangle=|5^2S_{1/2},F=1,m_F=1\rangle$, $|2\rangle=|5^2P_{1/2},F=2,m_F=0\rangle$, and $|4\rangle=|5^2P_{1/2},F=1,m_F=0\rangle$.

Under electric-dipole and rotating-wave approximations, the equations of motion for the density matrix governing atomic dynamics are

$$i\frac{\partial}{\partial t}\sigma_{11}-i\Gamma_{14}\sigma_{44}+\Omega_p^*\sigma_{41}-\Omega_p\sigma_{41}^*=0, \tag{1a}$$

$$i\frac{\partial}{\partial t}\sigma_{22}-i\Gamma_{24}\sigma_{44}+\Omega_s^*\sigma_{42}-\Omega_s\sigma_{42}^*=0, \tag{1b}$$

$$i\frac{\partial}{\partial t}\sigma_{33}-i\Gamma_{34}\sigma_{44}+\Omega_c^*\sigma_{43}-\Omega_c\sigma_{43}^*=0, \tag{1c}$$

$$i\frac{\partial}{\partial t}\sigma_{44}+i\Gamma_4\sigma_{44}-\Omega_p^*\sigma_{41}+\Omega_p\sigma_{41}^*-\Omega_s^*\sigma_{42}+\Omega_s\sigma_{42}^*-\Omega_c^*\sigma_{43}+\Omega_c\sigma_{43}^*=0, \tag{1d}$$

for diagonal density matrix elements and

$$\left(i\frac{\partial}{\partial t}+d_{21}\right)\sigma_{21}+\Omega_s^*\sigma_{41}-\Omega_p\sigma_{42}^*=0, \tag{2a}$$

$$\left(i\frac{\partial}{\partial t}+d_{31}\right)\sigma_{31}+\Omega_c^*\sigma_{41}-\Omega_p\sigma_{43}^*=0, \tag{2b}$$

$$\left(i\frac{\partial}{\partial t}+d_{32}\right)\sigma_{32}+\Omega_c^*\sigma_{42}-\Omega_s\sigma_{43}^*=0, \tag{2c}$$

$$\left(i\frac{\partial}{\partial t}+d_{41}\right)\sigma_{41}+\Omega_p(\sigma_{11}-\sigma_{44})+\Omega_s\sigma_{21}+\Omega_c\sigma_{31}=0, \tag{2d}$$

$$\left(i\frac{\partial}{\partial t}+d_{42}\right)\sigma_{42}+\Omega_s(\sigma_{22}-\sigma_{44})+\Omega_p\sigma_{21}^*+\Omega_c\sigma_{32}=0, \tag{2e}$$

$$\left(i\frac{\partial}{\partial t}+d_{43}\right)\sigma_{43}+\Omega_c(\sigma_{33}-\sigma_{44})+\Omega_p\sigma_{31}^*+\Omega_s\sigma_{32}^*=0, \tag{2f}$$

for nondiagonal density matrix elements, where $\Omega_p=\mathbf{e}_p\cdot\mathbf{d}_{14}\mathcal{E}_p/\hbar$, $\Omega_s=\mathbf{e}_s\cdot\mathbf{d}_{24}\mathcal{E}_s/\hbar$, and $\Omega_c=\mathbf{e}_c\cdot\mathbf{d}_{34}\mathcal{E}_c/\hbar$ are, respectively, half Rabi frequencies of the probe, signal, and control fields with $\mathbf{d}_{ij}\equiv\langle i|\mathbf{d}|j\rangle$ being density-matrix elements related to states $|i\rangle$ and $|j\rangle$; $d_{ij}=(\Delta_i-\Delta_j)+i\gamma_{ij}$ with $\Delta_4=\omega_p-(\omega_4-\omega_1)$ and $\Delta_3=\omega_p-\omega_c-(\omega_3-\omega_1)$ being, respectively, one- and two-photon detunings; $\gamma_{ij}=\frac{1}{2}(\Gamma_i+\Gamma_j)+\gamma_{ij}^{\text{col}}$ with $\Gamma_j=\sum_{i<j}\Gamma_{ij}$ denoting the total spontaneous emission decay rate of state $|j\rangle$, and γ_{jl}^{col} denoting the dephasing rate reflecting the loss of phase coherence between $|j\rangle$ and $|l\rangle$ without changing of population, as might occur with elastic collisions.

The equations of motion for Rabi frequencies of the probe- and signal-fields can be obtained by the Maxwell equation, which under slowly varying envelope approximation gives

$$i\left(\frac{\partial}{\partial z}+\frac{1}{c}\frac{\partial}{\partial t}\right)\Omega_p+\kappa_{14}\sigma_{41}=0, \tag{3a}$$

$$i\left(\frac{\partial}{\partial z}+\frac{1}{c}\frac{\partial}{\partial t}\right)\Omega_s+\kappa_{24}\sigma_{42}=0, \tag{3b}$$

where $\kappa_{14}=\mathcal{N}_a\omega_p|\mathbf{e}_p\cdot\mathbf{d}_{14}|^2/(2\epsilon_0c\hbar)$ and $\kappa_{24}=\mathcal{N}_a\omega_s|\mathbf{e}_p\cdot\mathbf{d}_{24}|^2/(2\epsilon_0c\hbar)$, with $\mathcal{N}_a$ being the atomic concentration and $\kappa_{14}\approx\kappa_{24}\equiv\kappa$. When deriving Eq. (3) we have assumed that (i) Ω_p and Ω_s are of the same order and much smaller than Ω_c, we can consider Ω_c as a constant in the system and (ii) both $\mathbf{k}_p$ and $\mathbf{k}_s$ are along the z-direction.

We assume that the atoms are initially populated in the states $|1\rangle$ and $|2\rangle$ (represented by the solid circles in the ground states $|1\rangle$ and $|2\rangle$ of Fig. 1). In the linear regime the probe and signal fields are very weak and the ground states not depleted during evolution, i.e. $\sigma_{11}^{(0)}+\sigma_{22}^{(0)}\approx1$ and $\sigma_{jj}^{(0)}\approx\sigma_{mn}^{(0)}\approx0$ (j=3, 4; m,n=1,2,3,4 with $m\neq n$). In this situation Maxwell–Bloch equations (1)–(3) can be linearized and support the solution $\Omega_p=F\exp\{i[K_p(\omega)z-\omega t]\}$ and $\Omega_s=G\exp\{i[K_s(\omega)z-\omega t]\}$ with F and G being constants. Here

$$K_p(\omega)=\frac{\omega}{c}+\kappa\frac{(\omega+d_{31})\sigma_{11}^{(0)}}{|\Omega_c|^2-(\omega+d_{31})(\omega+d_{41})}, \tag{4a}$$

$$K_s(\omega)=\frac{\omega}{c}+\kappa\frac{(\omega+d_{32})\sigma_{22}^{(0)}}{|\Omega_c|^2-(\omega+d_{32})(\omega+d_{42})}, \tag{4b}$$

are, respectively, the linear dispersion relations of the probe and the signal fields.

Fig. 2(a) shows the absorption curves $\text{Im}(K_p)$ for the probe field (solid line) and $\text{Im}(K_s)$ for the signal field (dotted line) as functions of ω by taking $\Omega_c=0$. Corresponding dispersion curves $\text{Re}(K_p)$ for the probe field (solid line) and $\text{Re}(K_s)$ for the signal field

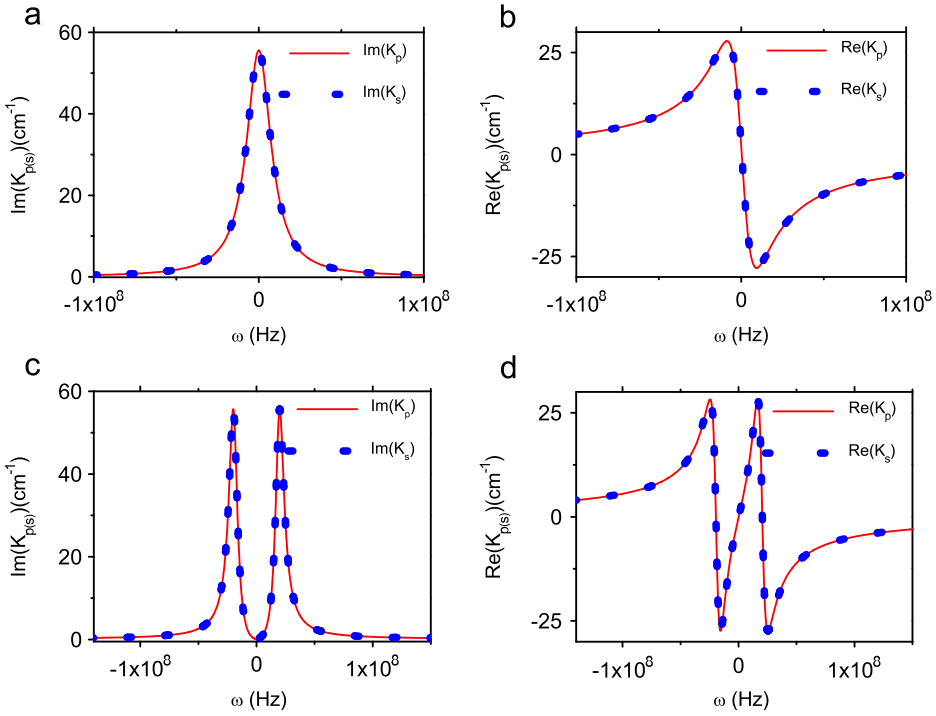

Fig. 2. (a) Absorption curves $\mathrm{Im}(K_p)$ for the probe field (solid line) and $\mathrm{Im}(K_s)$ for the signal field (dotted line) as functions of ω when $\Omega_c=0$. (b) Dispersion curves $\mathrm{Re}(K_p)$ for the probe field (solid line) and $\mathrm{Re}(K_s)$ for the signal field (dotted line) as a function of ω for the case of $\Omega_c=0$. (c) and (d) The case for $\Omega_c=20$ MHz.

(dotted line) as a function of ω are plotted in Fig. 2(b). The system considered is a cold ^{87}Rb atomic gas with the upper level in Fig. 1 as $5P_{1/2}$, while the lower levels as hyperfine magnetic sublevels of $5S_{1/2}$. System parameters are given by $\Gamma_{14}=\Gamma_{24}=\Gamma_{34}\simeq 6$ MHz, and $\Delta_3=\Delta_4=0$. One sees that for $\Omega_c=0$ there is only a single peak appearing in the absorption curve $\mathrm{Im}(K_p)$ and $\mathrm{Im}(K_s)$. However, when increasing Ω_c to $\Omega_c=20$ MHz, an EIT transparency window is opened in the region around $\omega=0$ in the absorption spectrum of both the probe and signal fields (panel (c)); simultaneously, a drastic change of dispersions (and hence a drastic reduction of group velocities) occurs (panel (d)). In addition, due to the symmetry of two Λ-configurations inherent in Fig. 1, the absorption and dispersion curves for both the probe and signal fields nearly coincide with each other. Especially, the group velocities of the probe and signal fields are perfectly matched. Such phenomena are the essential features of DEIT, which has many important applications in quantum computation and quantum information [6–11].

3. Mechanical analog of DEIT

We first consider a mechanical analog of DEIT. Our model is shown in Fig. 3, where two mass points of masses m_1 and m_2 are attached to two springs with spring constants κ_1 and κ_2, which are attached to a rigid support on the left hand side. The other side of these two mass points are attached separately by two springs with spring constants κ_{13} and κ_{23}, and then connected together to attach to the third mass point of mass m_3. The right hand side of the third mass point is attached to a spring with spring constant κ_3, which is attached to another rigid support on the right side. We assume in the system that the mass points m_1 and m_2 are, respectively, driven by two harmonic forces $F_1e^{-i\omega t}+$c.c. and $F_2e^{-i\omega t}+$c.c., and all three mass points put on horizontal solid walls that contribute friction force to them. Obviously, the system is a setting with three coupled linear harmonic oscillators with deriving and damping.

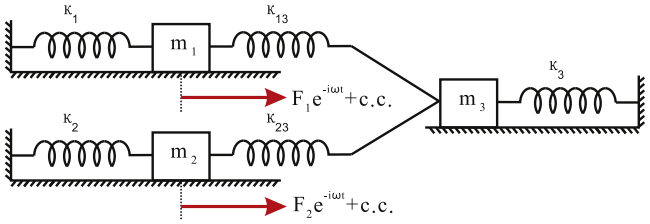

Fig. 3. Mechanical model used to simulate DEIT. m_j is the mass of jth harmonic oscillator with κ_j ($j=1,2,3$), κ_{13}, and κ_{23} being spring constants. Arrows below m_1 and m_2 indicate harmonic forces $F_1e^{-i\omega t}+$c.c. and $F_1e^{-i\omega t}+$c.c., respectively.

To describe the classical motion of this system, we use one-dimensional coordinate x_j ($j=1,2,3$) to represent the displacement of jth harmonic oscillator deviating from its equilibrium position. The equations of motion for harmonic oscillators are

$$\ddot{x}_1(t)+\gamma_1\dot{x}_1(t)+\omega_1^2x_1(t)-\Omega_c^2x_3(t)=(F_1/m_1)e^{-i\omega t}+\text{c.c.}, \tag{5a}$$

$$\ddot{x}_2(t)+\gamma_2\dot{x}_2(t)+\omega_2^2x_2(t)-\Omega_r^2x_3(t)=(F_2/m_2)e^{-i\omega t}+\text{c.c.}, \tag{5b}$$

$$\ddot{x}_3(t)+\gamma_3\dot{x}_3(t)+\omega_3^2x_3(t)-\Omega_c^2x_1(t)-\Omega_r^2x_2(t)=0, \tag{5c}$$

where the dot over x_j denotes time derivative, $\omega_1^2=(\kappa_1+\kappa_{13})/m_1$, $\omega_2^2=(\kappa_2+\kappa_{23})/m_2$, $\omega_3^2=(\kappa_3+\kappa_{13}+\kappa_{23})/m_3$, $\Omega_c^2=\kappa_{13}/m_1$, and $\Omega_r^2=\kappa_{23}/m_2$. γ_j is the damping constant of jth harmonic oscillator, resulted by the friction force by the horizontal solid wall.

We assume that the solution of Eqs. (5) has the form $x_j=N_je^{-i\omega t}+$c.c. ($j=1,2,3$), with N_j being constant. Then it is easy to obtain

$$x_j=-\frac{A_j}{B_j}e^{-i\omega t}+\text{c.c.}\quad(j=1,2), \tag{6}$$

where $A_1=F_1(D_2D_3-\Omega_r^4)/m_1+F_2\Omega_c^2\Omega_r^2/m_2$, $B_1=\Omega_c^4D_2+(\Omega_r^4-D_2D_3)D_1$, $A_2=F_1D_3/m_1+(\Omega_c^4-D_1D_3)[F_1(\Omega_r^4-D_2D_3)/m_1]-F_2\Omega_c^2\Omega_r^2/m_2$, $B_2=\Omega_c^2\Omega_r^2[\Omega_c^4D_2+(\Omega_r^4-D_2D_3)D_1]$, with $D_j=\omega_j^2-\omega^2+i\gamma_j\omega$ ($j=1,2,3$).

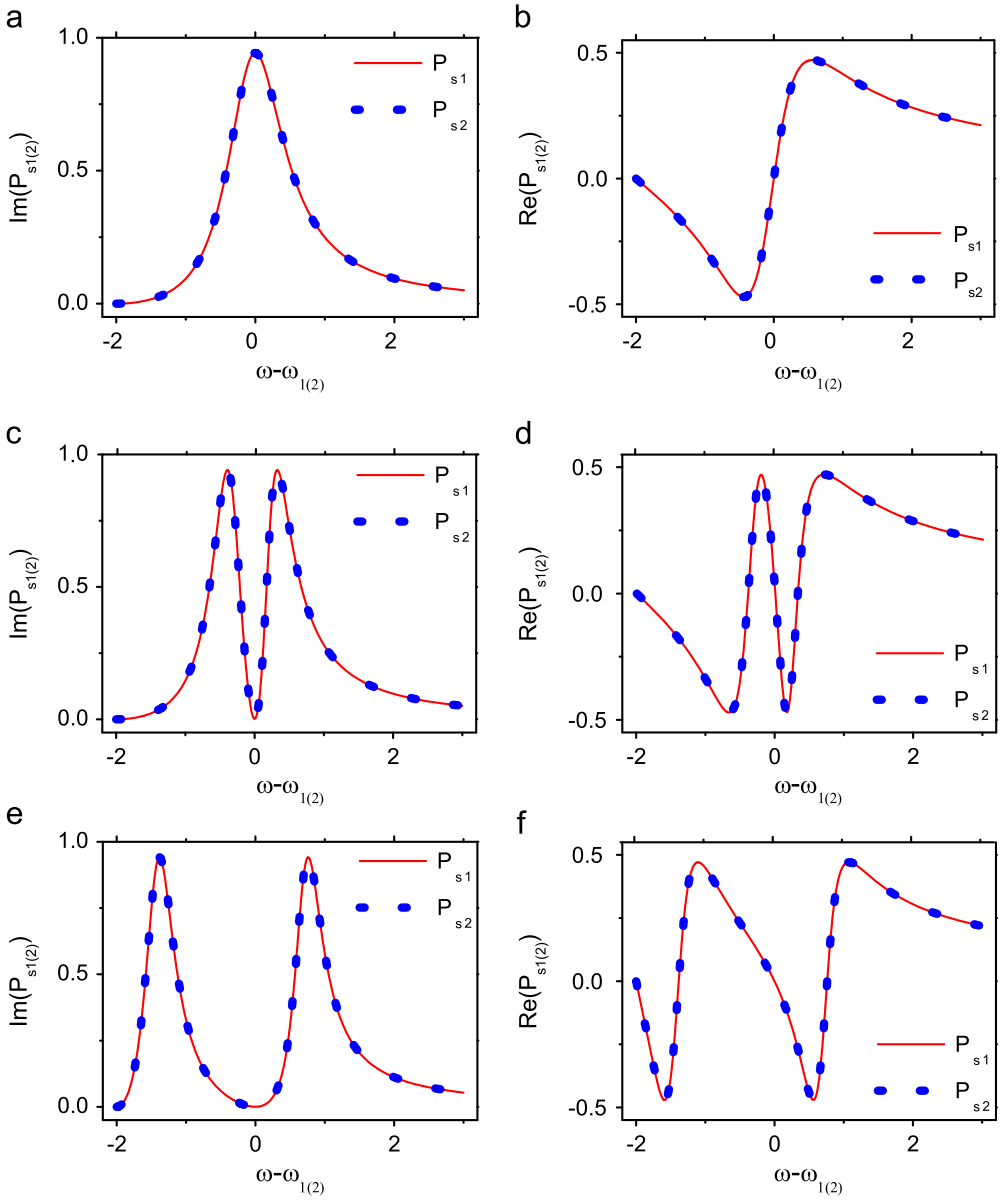

Fig. 4. (a) The solid (dotted) line is the absorption spectrum $\mathrm{Im}(P_{s1})$ ($\mathrm{Im}(P_{s2})$) as a function of $\omega-\omega_1$ ($\omega-\omega_2$) when $\Omega_c=0.01$. (b) Corresponding real part $\mathrm{Re}(P_{s1})$ ($\mathrm{Re}(P_{s2})$) for the case of $\Omega_c=0.01$. (c) and (d) The case for $\Omega_c=1.0$. (e) and (f) The case for $\Omega_c=1.6$.

The mechanical powers $P_1(t)$ and $P_2(t)$ absorbed, respectively, by the harmonic oscillators 1 and 2 from the external driving forces can be calculated by the formulas

$$P_j(t)=(F_j e^{-i\omega t}+\text{c.c.})\dot{x}_j(t) \quad (j=1,2). \tag{7}$$

The average of powers during one period of oscillation are respectively given by

$$P_{sj}(\omega)=\frac{\int_0^{2\pi/\omega}P_j(t)\,\mathrm{d}t}{2\pi/\omega} \quad (j=1,2). \tag{8}$$

The solid line shown in Fig. 4(a) is the absorption spectrum $\mathrm{Im}(P_{s1})$ ($\mathrm{Im}(P_{s2})$) as a function of $\omega-\omega_1$ ($\omega-\omega_2$) for $\Omega_c=0.01$. The panel (b) is the corresponding real part $\mathrm{Re}(P_{s1})$ ($\mathrm{Re}(P_{s2})$). One sees that for this small Ω_c there is only a single peak appearing in the absorption curves $\mathrm{Im}(P_{s1})$ and $\mathrm{Im}(P_{s2})$. However, when increasing Ω_c to $\Omega_c=1.0$, an "EIT" transparency window opens in the curves of $\mathrm{Im}(P_{s1})$ and $\mathrm{Im}(P_{s2})$ (panel (c)), with the real part $\mathrm{Re}(P_{s1})$ and $\mathrm{Re}(P_{s2})$ changed greatly (panel (d)). The panels (e) and (f) are the case for $\Omega_c=1.6$, in which case the transparency window opens more wide. When plotting the figure we have taken system parameters $\kappa_1=\kappa_2=\kappa_{13}=\kappa_{23}=\kappa_3=\kappa$, $m_1=m_2=m_3=m$, $\Omega_c=\Omega_r$, and $\gamma_1=\gamma_2=1.0$ and $\gamma_3=1.0\times10^{-3}$, and $\omega_1=\omega_2=\omega_3=2.0$ (all quantities have the dimension of frequency). The values of F_1/m and F_2/m are taken to be 0.1 in force per mass units.

Compared with Figs. 4 and 2, we see that the system of the present coupled-oscillator system has the DEIT property similar to that of the tripod-type four-level atomic system described in the last section. The physical reason of the existence of DEIT in the coupled harmonic system can be explained as follows. It is well known [25] that the energy absorbed by a damped harmonic oscillator driven by an external force is a function of driving frequency. In the case of our system (Fig. 3), the damped oscillators m_1 and m_2 are driven by the harmonic forces $F_1e^{-i\omega t}+\text{c.c.}$ and $F_2e^{-i\omega t}+\text{c.c.}$ Standard absorption resonances for the both oscillators are observed for small κ_{13} and κ_{23} (and hence small Ω_c and Ω_r) (Fig. 4(a)). However, when the oscillator

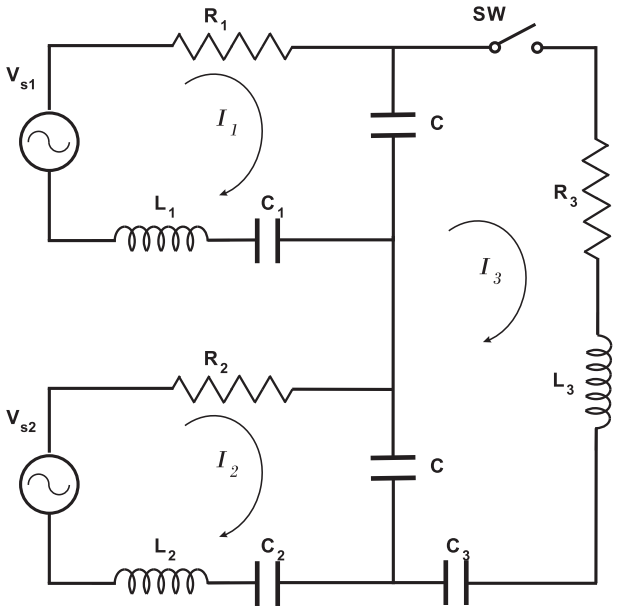

Fig. 5. Coupled RLC electrical circuit used to model the tripod-type 4-level atomic system. R_j, C_j, L_j, and V_{sj} are, respectively, the resister, capacitor, inductor, and alternating voltage source of the jth loop. C is the capacitor shared by 1–3 and 2–3 loops, and SW is a switch of the loop 3.

m_3 moves with large κ_{13} and κ_{23} (and hence large Ω_c and Ω_r), the absorptions of the oscillators m_1 and m_2 are suppressed, and thus "EIT" transparency windows open in the both absorption spectra (Fig. 4(c) and (e)). Consequently, we can make the following analog: (i) In our mechanical model, the spring with spring constant κ_{13} and the spring with spring constant κ_{23} emulate the control field Ω_c that couples the states $|3\rangle$ and $|4\rangle$ in Fig. 1; (ii) Two harmonic driving forces $F_1e^{-i\omega t}+$c.c. and $F_2e^{-i\omega t}+$c.c. acting on the oscillators m_1 and m_2 emulate the probe field and the signal field in Fig. 1, respectively; and (iii) The damping constants in Eq. (5) emulate the decay rates of spontaneous emission from the excited state to three lower states of Fig. 1. Thus, by changing the "control-field Rabi frequency" Ω_c and Ω_r, one can realize a (mechanical) DEIT in the system.

4. Electrical analog of DEIT

A driven and damped harmonic oscillator has a well-known correspondence with an electrical circuit consisting of a resistor R, an inductor L and a capacitor C connected in series to an alternating voltage source V. RLC circuits are easy to build in laboratory and may be used as excellent examples of non-mechanical oscillations. We used such circuits to study DEIT by analyzing the absorption of electric power in resistances. The electric analog to the atomic system of Fig. 1 is shown in Fig. 5, where the loop of circuit composed of the inductor L_3 and capacitors C_3 and C is a control oscillator. The resistor R_3 accounts for the spontaneous radiative decay from the state $|4\rangle$ to the state $|3\rangle$. Atoms are modeled by using two loops, each of them composed of one inductor, two capacitors, and one resistor, i.e. $L_1C_1R_1$ and $L_2C_2R_2$. Here R_1 and R_2 determine the spontaneous radiative decays from the upper state $|4\rangle$ to lower states $|1\rangle$ and $|2\rangle$, respectively. The capacitor C shared between loops 1 and 3 and loop 2 and 3 models the coupling between atoms and the control field. Two probe fields are modeled by frequency-tunable voltage sources V_{s1} and V_{s2}.

The DEIT is investigated by examining the frequency dependence on the transmitted power from frequency-tunable voltage sources $V_{s1}e^{-i\omega t}+$c.c. and $V_{s2}e^{-i\omega t}+$c.c. to the first and second loops. If the electric currents in three loops are, respectively, written as $I_1(t)=\dot{q}_1(t)$, $I_2(t)=\dot{q}_2(t)$, $I_3(t)=\dot{q}_3(t)$, we obtain the following coupled equations:

$$\ddot{q}_1(t)+r_1\dot{q}_1(t)+\omega_1^2q_1(t)-\Omega_c^2q_3(t)=(V_{s1}/L_1)e^{-i\omega t}+\text{c.c.}, \tag{9a}$$

$$\ddot{q}_2(t)+r_2\dot{q}_2(t)+\omega_2^2q_2(t)-\Omega_r^2q_3(t)=(V_{s2}/L_2)e^{-i\omega t}+\text{c.c.}, \tag{9b}$$

$$\ddot{q}_3(t)+r_3\dot{q}_3(t)+\omega_3^2q_3(t)-\Omega_c^2q_1(t)-\Omega_r^2q_2(t)=0, \tag{9c}$$

where $r_j=R_j/L_j$, $\omega_j^2=1/(L_jC_{ej})$ $(j=1,2,3)$, $\Omega_c^2=1/(L_1C)$, and $\Omega_r^2=1/(L_2C)$, with effective capacitances given by $C_{e1}=CC_1/(C+C_1)$, $C_{e2}=CC_2/(C+C_2)$, and $C_{e3}=(C/2)C_3/(C/2+C_3)$.

It is easy to get the solution of Eq. (9)

$$q_j=-\frac{U_j}{W_j}e^{-i\omega t}+\text{c.c.}\quad (j=1,2). \tag{10}$$

Here $U_1=V_{s1}(D_2D_3-\Omega_r^4)/L_1+V_{s2}\Omega_c^2\Omega_r^2/L_2$, $W_1=\Omega_c^4D_2+(\Omega_r^4-D_2D_3)D_1$, $U_2=V_{s1}D_3/L_1+(\Omega_c^4-D_1D_3)[V_{s1}(\Omega_r^4-D_2D_3)/L_1]-V_{s2}\Omega_c^2\Omega_r^2/L_2$, and $W_2=\Omega_c^2\Omega_r^2[\Omega_c^4D_2+(\Omega_r^4-D_2D_3)D_1$, with $D_j=\omega_j^2-\omega^2+ir_j\omega$ $(j=1,2,3)$.

The electric power $P_j(t)$ transferred from the voltage source V_{sj} to the resonant electric circuit $L_jC_jR_j$ is given by $P_{sj}(t)=(V_{sj}e^{-i\omega t}+\text{c.c.})\dot{q}_j(t)$. The average of the electric power $P_{sj}(t)$ during one period of oscillation reads as

$$P_{sj}(\omega)=\frac{\int_0^{2\pi/\omega}(V_{sj}e^{-i\omega t}+\text{c.c.})\dot{q}_j(t)\,dt}{2\pi/\omega}\quad (j=1,2). \tag{11}$$

Using Eq. (10) we can obtain the concrete expression of $P_{sj}(\omega)$, which are omitted here for saving space.

Fig. 6(a) shows the absorption spectrum $\text{Im}(P_{s1})$ ($\text{Im}(P_{s2})$) as a function of $\omega-\omega_1$ ($\omega-\omega_2$) for $\Omega_c=0.01$. The corresponding real part $\text{Re}(P_{s1})$ (solid line) and $\text{Re}(P_{s2})$ (dotted line) are plotted in panel (b). In this case, only a single peak appears in the curves of $\text{Im}(P_{s1})$ and $\text{Im}(P_{s2})$. When increasing Ω_c, the curves undergo a drastic change. In fact, a doublet appears in the absorption spectra. Shown in the panel (c) is the case for $\Omega_c=1.0$. We see that in the region around $\omega-\omega_1=0$ ($\omega-\omega_2=0$) an "EIT" transparency window opens. Simultaneously, the real part $\text{Re}(P_{s1})$ and $\text{Re}(P_{s2})$ change drastically (see the panel (d)). The panels (e) and (f) are the case for $\Omega_c=1.6$, in which case the transparency window becomes more wide. When plotting the figure we have taken system parameters $\gamma_1=\gamma_2=1.0$ and $\gamma_3=1.0\times10^{-3}$, and $\omega_1=\omega_2=\omega_3=2.5$ (all quantities have dimension of frequency). The values of V_{s1}/L_1 and V_{s2}/L_2 are taken to be 0.1 in voltage per inductance units. Obviously, the phenomenon demonstrated here is also very similar to the DEIT appeared in the tripod-type four-level atomic system described in Section 2.

5. Conclusion

In this paper, the DEIT in a tripod-type four-level atomic system has been modeled by two classical systems. The first is a set of three coupled harmonic oscillators subject to frictional forces and external drives and the second is a set of three coupled RLC circuits with electric resistors and alternating voltage sources. We have shown that both of the two classical systems have linear absorption spectrum very similar to that of the four-level tripod-type atomic system. These classical analogies provide simple and intuitive physical description of quantum interference processes and can be used to illustrate experimental observations of the DEIT in quantum systems. A further interesting topic is to consider possible analogs in nonlinear regime, where cross-Kerr nonlinearity will appear.

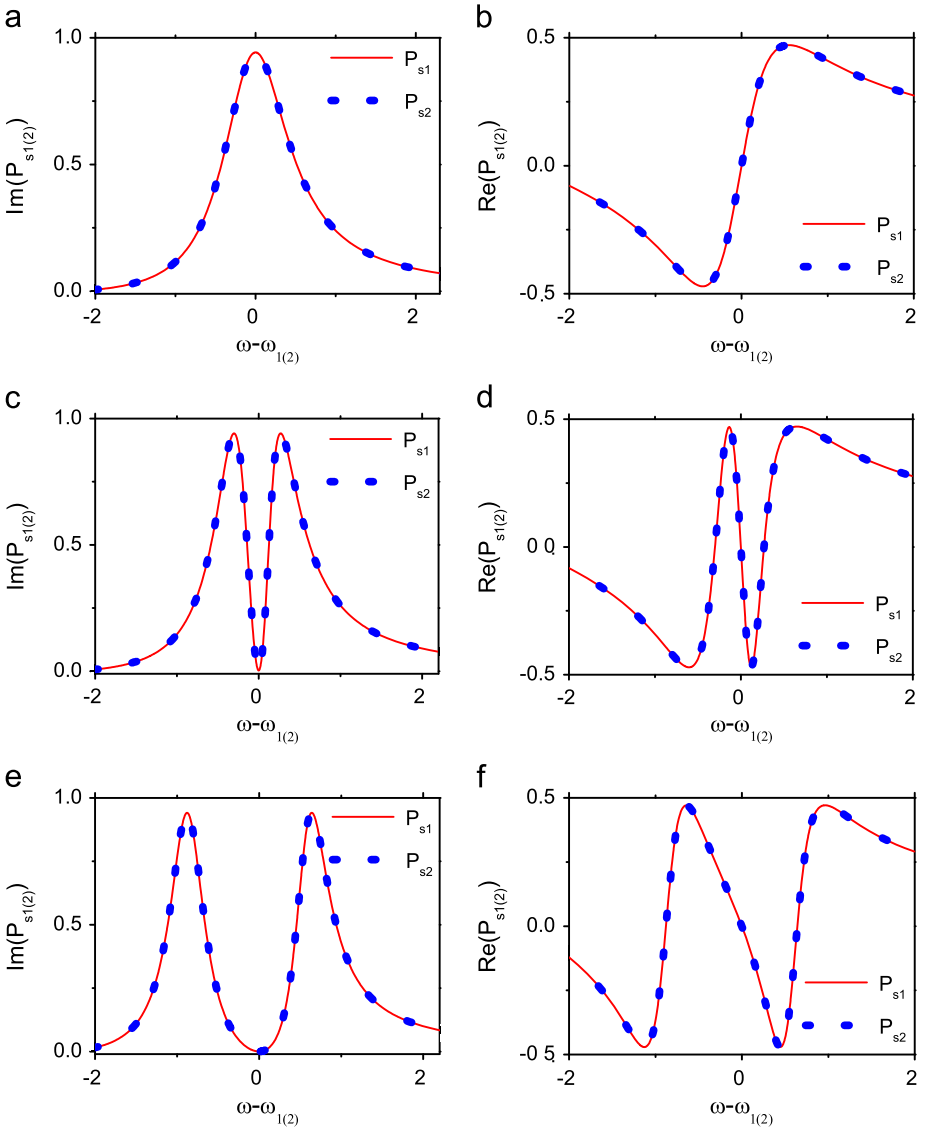

Fig. 6. (a) The solid (dotted) line is the absorption spectrum $\mathrm{Im}(P_{s1})$ ($\mathrm{Im}(P_{s2})$) as a function of $\omega-\omega_1$ ($\omega-\omega_2$) for $\Omega_c=0.01$. (b) Corresponding real part $\mathrm{Re}(P_{s1})$ ($\mathrm{Re}(P_{s2})$) for $\Omega_c=0.01$. (c) and (d) The case for $\Omega_c=1.0$. (e) and (f) The case for $\Omega_c=1.6$.

Acknowledgments

This work was supported by NSF-China under Grant numbers 10874043, 11174080, and 11105052, and by the Open Fund from the State Key Laboratory of Precision Spectroscopy, ECNU.

References

[1] M. Fleischhauer, A. Imamoglu, J.P. Marangos, Review of Modern Physics 77 (2005) 633.
[2] K.B. Khurgin, R.S. Tucker (Eds.), Slow Light: Science and Applications, CRC, Taylor and Francis, Boca Raton, 2009.
[3] Y. Wu, L. Deng, Physical Review Letters 93 (2004) 143904.
[4] G. Huang, L. Deng, M.G. Payne, Physical Review E 72 (2005) 016617.
[5] H.-j. Li, Y.-p. Wu, G. Huang, Physical Review A 84 (2011) 033816.
[6] D. Petrosyan, Y.P. Malakyan, Physical Review A 70 (2004) 023822.
[7] S. Rebi, et al., Physical Review A 70 (2004) 032317.
[8] Z.-B. Wang, K.-P. Marzlin, B.C. Sanders, Physical Review Letters 97 (2006) 063901.
[9] A. MacRae, G. Campbell, A.I. Lvovsky, Optics Letters 33 (2008) 2659.
[10] S. Li, et al., Physical Review Letters 101 (2008) 073602.
[11] C. Hang, G. Huang, Journal of the Optical Society of America B 26 (2009) 413.
[12] M.A. Nielsen, I.L. Chuang, Quantum Computation and Quantum Information, Cambridge University Press, Cambridge, 2000.
[13] D. Dragoman, M. Dragoman, Quantum-Classical Analogies, Springer, Berlin, 2004.
[14] P.R. Hemmer, M.G. Prentiss, Journal of the Optical Society of America B 5 (1988) 1613.
[15] Y. Zhu, et al., Physical Review Letters 64 (1990) 2499.
[16] B.W. Shore, et al., American Journal of Physics 77 (2009) 1183.
[17] S. Zhang, et al., Physical Review Letters 101 (2008) 047401.
[18] Z. Han, S.I. Bozhevolnyi, Optics Express 19 (2011) 3251–3257.
[19] J. Wu, et al., Applied Physics Letters 99 (2011) 161113.
[20] N. Papasimakis, et al., Applied Physics Letters 94 (2009) 211902.
[21] N. Liu, et al., Nano Letters 10 (2010) 1103.
[22] C. Kurter, et al., Physical Review Letters 107 (2011) 043901.
[23] C.L.G. Alzar, M.A.G. Martinez, P. Nussenzveig, American Journal of Physics 70 (2002) 37.
[24] J. Harden, A. Joshi, J.D. Serna, European Journal of Physics 32 (2011) 541, The system studied in this work has two control fields and one probe field, and hence is different from our system.
[25] L.D. Landau, E.M. Lifshitz, Mechanics, 3rd ed., Butterworth-Heinemann, Oxford, 2002.